ACS APPLIED POLYMER MATERIALS

pubs.acs.org/acsapm Article

Synthesis and Self-Assembly of Block Polyelectrolyte Membranes through a Mild, 2-in-1 Postpolymerization Treatment

David J. Goldfeld,[‡] Eric S. Silver,[‡] Madalyn R. Radlauer, and Marc A. Hillmyer*

Cite This: *ACS Appl. Polym. Mater.* 2020, 2, 817−825 Read Online

ABSTRACT: Block polymer systems containing spatially separated positive and negative charges are desirable for a number of applications, including biomedical devices, membrane separations, and coatings. Unfortunately, the tendency of positive and negative block polymers to charge cancel and form an insoluble coacervate precipitate leads to processing difficulties in the fabrication of charged thin films. We use postpolymerization modifications to simultaneously add both negative and positive charges to self-assembled neutral ABC triblock polymer thin films. Using reversible addition−fragmentation chain transfer polymerization, we synthesized triblock terpolymers consisting of poly(*n*-propyl styrene sulfonic ester), poly(4-chlorostyrene), and poly(vinylbenzyl chloride). The chemical functionalization of both charged blocks was accomplished simultaneously through exposure to gaseous trimethylamine in a single step at room temperature, simplifying the synthetic procedure and preserving the microstructure of the thin film. The quantitative functionalization was tracked through attenuated total reflectance infrared spectroscopy, and the thin film morphology was evaluated using intermodulation atomic force microscopy, transmission electron microscopy, and grazing-incidence small-angle X-ray scattering.

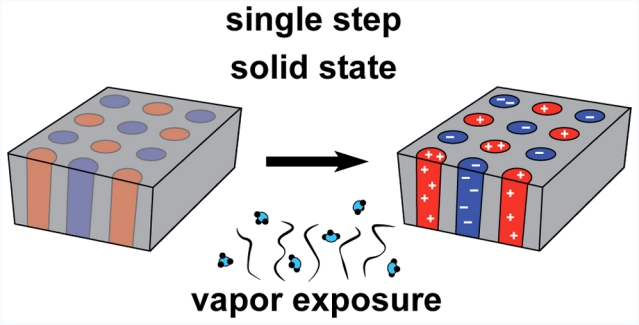

KEYWORDS: *block polymers, polyelectrolyte, thin film, polyampholyte, self-assembly, postpolymerization modification, atomic force microscopy*

INTRODUCTION

Polyelectrolytes are polymers containing fixed charges along the length of the polymer chain.[1,2] Both polyanions and polycations are used for a variety of applications, including battery materials,[3] membrane separations,[4] and biomedical devices.[5] Due to their broad applicability, polyelectrolytes have been studied extensively in terms of their solution self-assembly,[6] network formation and swelling behavior,[7,8] and interfacial phenomena.[9] More recent work includes studies on block polyelectrolytes, which are polymer chains with covalently linked, chemically distinct blocks of a polyelectrolyte segment connected to a neutral block in a variety of architectures, including A−B diblock polymers, A−B−A triblock polymers, and other multiblocks.[10−13]

A polyampholyte is a polyelectrolyte that contains both negative and positive charges on separate monomers within the polymer chain.[14,15] A subset of this polymer class is block polyampholytes, where blocks of polyanions are covalently attached to blocks of polycations. These have been investigated for their phase behavior in solution, including the formation of complex coacervates with additives like pharmaceuticals and genetic material leading to nanoparticle self-assembly.[10−13] Despite studies into the solution-state behavior of these systems, the solid-state assembly of block polyampholytes has been relatively unexplored.[16−18] Applications that would benefit from spatially separated positively and negatively charged polymer domains include antibiofouling coatings, separation membranes, and selective physical adsorption of anionic and cationic targets to surfaces.[3,19] For example, in wastewater treatment, a common issue when using reverse osmosis (RO) membranes is that as more water is filtered, the water remaining on the high-pressure side increases in concentration, leading to both higher incidences of scaling (buildup of salt precipitates on the membranes) and higher osmotic pressure resulting in increased pressure and energy requirements. A membrane capable of piezodialysis being incorporated periodically into the purification route would help to decrease the salt concentration in the water feed, thereby decreasing the energy needs of the water plant and also decreasing scaling and thus extending the lifetimes of RO membranes. According to theory, smaller domain spacings lead to higher fluxes of salts through the membranes, improving

Received: November 18, 2019
Accepted: January 10, 2020
Published: January 23, 2020

https://dx.doi.org/10.1021/acsapm.9b01100
ACS Appl. Polym. Mater. 2020, 2, 817−825

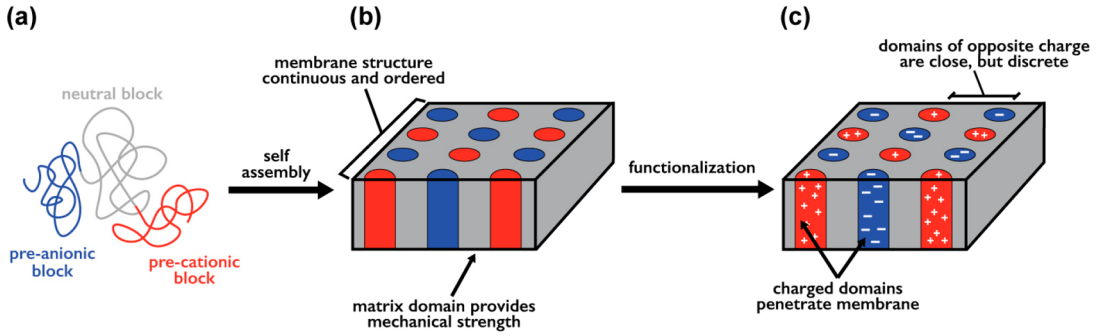

Figure 1. Schematic of (a) a neutral triblock polymer and subsequent self-assembly into (b) a thin film with cylinder-on-square lattice morphology. The thin film is then functionalized to yield (c) an ordered array of spatially separated positively and negatively charged domains.

energy efficiency. While previous systems have been fabricated with domain spacings on the micron scale, further reduction of the charged domains to the nanometer scale should lead to increased ion fluxes.[20−22] To achieve spatially separated nanoscale domains of opposite charge, we take advantage of block polymer self-assembly.[23,24] Self-assembled morphologies in thin films are an area of current interest,[24−27] and the behavior of block polyampholytes in thin films is largely unknown.

In the system described here, we separate the two charged blocks with a neutral spacer, so the films will maintain domains of a fixed positive charge separated from domains of a fixed negative charge, which we expect will display a number of distinctive behaviors compared to both zwitterionic systems (where a fixed positive and fixed negative charge are contained in a single monomer unit)[28] and polyelectrolyte complexes (which allow the fixed charges on different parts of the polymer chain to come together into a separate phase, releasing mobile ions into solution).[29,30]

Complex coacervation prevents the straightforward fabrication of self-assembled films containing spatially separated opposite charges. When a polyanion and polycation are in a solution together, the entropically driven release of counterions leads to a liquid−liquid macrophase separation into a phase rich in polymer and a supernatant rich in small molecule counterions.[21−34] These charge-canceled aggregates cannot segregate into separate domains as they form solid-state complexes, leading to a single domain of fixed positive and negative charges together, often as gels or solid precipitates.[7,35]

One possible way to self-assemble a microphase-separated structure of positive and negative charges in the solid state is to synthesize a neutral polymer that can later be functionalized to contain charges (Figure 1a). The neutral precursor polymer can be processed in common organic solvents, and self-assembly can be assisted using standard thin film practices, such as solvent vapor or thermal annealing (Figure 1b).[25] These systems can be characterized in the solid state using a variety of characterization techniques, including atomic force microscopy (AFM), transmission electron microscopy (TEM), grazing-incidence small-angle X-ray scattering (GISAXS), and attenuated total reflectance infrared (ATR-IR) spectroscopy.

After the neutral block polymer has assembled into a desired morphology, postpolymerization modification can be used to convert the domains to their respective charged species (Figure 1c). Such strategies have been demonstrated in the past for polymers in the solid state, but the modification strategies have typically used harsh reagents and conditions, for example exposure to pure sulfuric or chlorosulfonic acid at temperatures near or exceeding 100 °C.[16,17] These conditions are inefficient and can lead to large defects in the solid-state structures of the polymers, characterized by substantial changes in the morphology from the softening of the polymers and undesired chemical degradation.[16−18] In addition, it is often difficult or impossible to show the extent of conversion to charged groups, and these reactions generally fall short of quantitative conversion. Our goal is to use a system that is easily functionalized under mild conditions and can be readily monitored to quantify conversion.

Once the polymer is functionalized in the solid state, the polyelectrolytes still suffer from a strong tendency to swell in the presence of water or high humidity.[16] The swelling allows the polyanion and polycation chains to move within the structure, which can lead to the loss of separation between the domains and the rearrangement of the morphology. To prevent this, we use a neutral, unreactive matrix B block in the center of an ABC triblock polymer system to contain the charged domains and keep them separated after functionalization to polyelectrolytes. Since the eventual applications often involve submersion of the membranes into water (where the charged polyelectrolytes are completely soluble), it is vital to have a glassy and hydrophobic support material with a glass transition temperature (T_g) much higher than room temperature to hold the membrane together and separate the positive and negative domains while they swell under osmotic pressure. One possible idealized morphology would be a cylinder-on-square lattice morphology,[36−38] which has a neutral B block separating alternating cylinders of the A and C charged blocks, consisting of first a polyanion domain, then a spacer, and then a polycation domain. The neutral B block needs to be chemically stable under the conditions of functionalization (mildly acidic/basic conditions). It is also advantageous for the support block to be processable in common solvents.

There are several commercially available derivatives of styrene that are negatively and positively charged like styrenesulfonate, 4-vinylbenzoic acid, and *N*,*N*,*N*-trimethyl-4-vinylanilium chloride. There are similarly a wide variety of substituted styrenes that are inert to many chemical transformations, including 4-methylstyrene, 4-*tert*-butylstyrene, and 4-chlorostyrene. Most of these styrene derivatives can be used to make polymers that are glassy at room temperature, and many of them are well studied and readily available.[39−41] The ideal system will have three blocks that are processable in similar solvents and have similar surface energies to simplify thin film self-assembly into the desired perpendicularly oriented morphologies. We achieved this by using a styrene backbone through all three blocks of the ABC triblock polymer

https://dx.doi.org/10.1021/acsapm.9b01100
ACS Appl. Polym. Mater. 2020, 2, 817−825

Scheme 1. Synthesis of Diblock and Triblock Polymers Using RAFT Polymerization to Yield AB, BC, and ABC Block Polymers Containing PSSE, PS, P4ClS, and PVBC

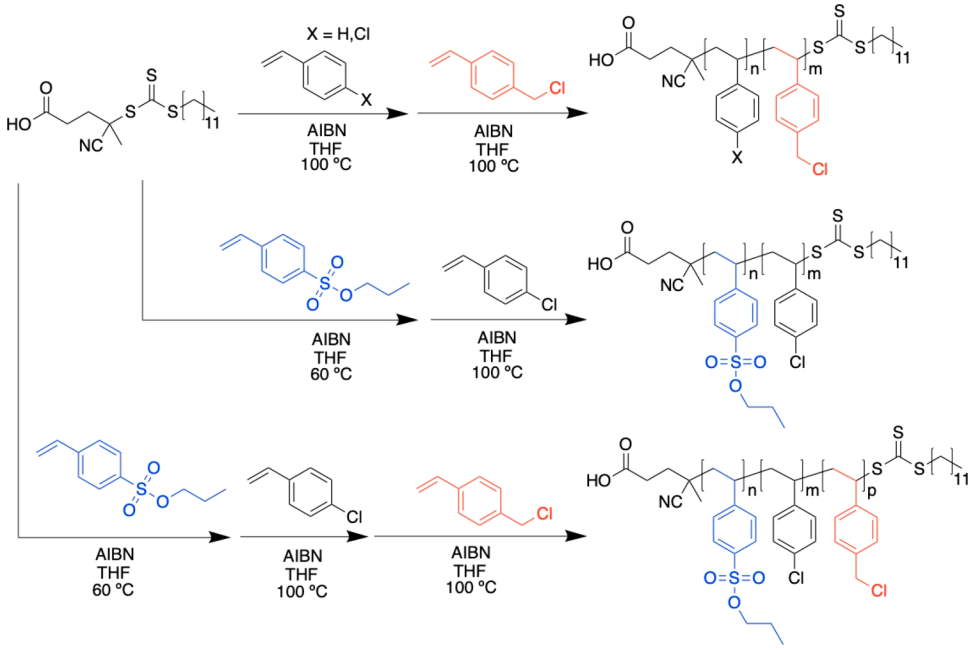

with covalently attached masked functional groups that are converted to anions and cations after polymerization. Herein, we detail the synthesis, solid-state conversion to polyanions and polycations, and self-assembly properties of a series of diblock and triblock polymers (Scheme 1).

RESULTS AND DISCUSSION

Pre-Cationic Block. Our target for the positively charged C block of the ABC polymer is an initially neutral polymer that can be functionalized postpolymerization to carry a permanent positive charge. One of the most commonly used polymers for this purpose is poly(vinylbenzyl chloride) (PVBC). Vinylbenzyl chloride (VBC) is a commercially available styrene derivative that contains a benzyl chloride functional group that is stable under radical polymerization conditions and can be functionalized with a variety of nucleophiles after polymerization. The most common functionalization is exposure of the PVBC to an amine.[42] Using a protected primary amine yields a pH-sensitive polycationic block,[43] and using a trialkylamine yields a poly(vinylbenzyl trialkylammonium chloride) (PVBAC) with positive fixed charges installed at every repeat unit.[44] PVBAC has been studied in a variety of applications,[45] including anion exchange membranes and gene delivery.[44,46] In addition, PVBC is ideal for our system since it is a stable, neutral polymer that is glassy at room temperature ($T_g \sim 108$ °C)[47,48] and soluble in a wide range of organic solvents. It can be polymerized in a controlled manner through radical addition−fragmentation chain transfer (RAFT) polymerization[49] techniques and adds easily onto styrenic macroinitiators to form block polymers with well-defined molar masses and low dispersities.[50]

PVBC is commonly copolymerized with styrene to form both statistical copolymers, i.e., the well-known Merrifield resins,[51] and to form block polymers of poly(styrene)-*b*-poly(vinylbenzyl chloride) or poly(vinylbenzyl chloride)-*b*-poly(styrene).[52−54] However, these polymers are typically converted to the charged ammonium state immediately after synthesis for the solution-state self-assembly of amphiphiles or solid-state ion-conductive membranes. As a result, the only evidence of the solid-state morphology of poly(styrene)-*b*-poly(vinylbenzyl chloride) in literature is a differential scanning calorimetry (DSC) study showing a merged T_g for a single sample without further investigating the effects of the molar mass or volume fraction on the diblock behavior.[47] We first investigated the solid-state self-assembly behavior of this diblock before incorporation into our target triblock polymers.

We initially synthesized a homopolymer of polystyrene through RAFT polymerization using a commercially available chain transfer agent (4-cyano-4-[(dodecylsulfanylthiocarbonyl)sulfanyl]pentanoic acid; CTA) and azobis(isobutyronitrile) (AIBN) as a radical thermal initiator. The initial block was then chain extended by growing a block of PVBC from the PS macroinitiator to yield PS_{140}−$PVBC_{140}$ (subscripts indicate the average degree of polymerization) with a molar mass (M_n) = 36 kg mol^{-1} and dispersity ($Đ$) = 1.32 (Figures S11 and S27; polymer sample data are summarized in Table S1). The isolated diblock was then evaluated for efficiency in converting the benzyl chloride functional group to a trimethylammonium group through exposure to trimethylamine (TMA) (Scheme 2). PVBC homopolymer could be functionalized by suspending it in a 45% by weight solution of TMA in water, where after functionalization to the charged state, the polymer dissolved. After isolating the PVBAC, Fourier-transform infrared spectroscopy (FTIR) showed the disappearance of the C−Cl wag and the emergence of the C−N stretch (Figure S62). Thin films (30−60 nm) of the diblock PS_{140}−$PVBC_{140}$ were then spin coated from chlorobenzene onto silicon wafers and then converted to PS_{140}−$PVBAC_{140}$ by exposure to TMA vapor in a sealed glass chamber (see SI for details on the spin coating and annealing recipes). Similarly, the IR band for the C−Cl wag at 1266 cm^{-1} disappeared, and the new C−N stretch at 1220 cm^{-1} appeared after 1 h of exposure (Figure S63).

https://dx.doi.org/10.1021/acsapm.9b01100
ACS Appl. Polym. Mater. 2020, 2, 817−825

Scheme 2. Conversion of the Neutral Homopolymers to Their Ionic Counterparts[a]

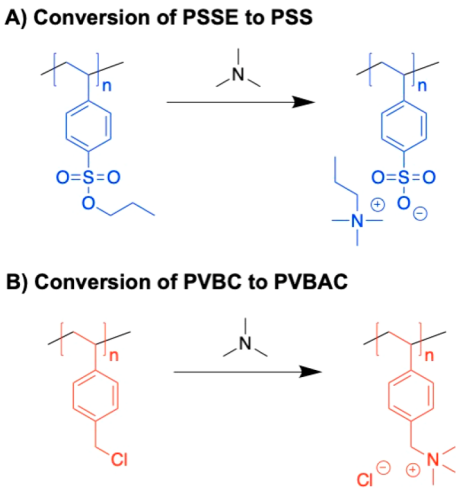

[a](A) Poly(*n*-propyl styrene sulfonic ester) (PSSE) is exposed to trimethylamine, and the propyl group undergoes an S_N2 reaction to form poly(styrene sulfonate) (PSS). (B) Poly(vinylbenzyl chloride) (PVBC) is exposed to trimethylamine, and the benzyl chloride functional group undergoes an S_N2 reaction to form poly(vinylbenzyl trimethylammonium chloride) (PVBAC).

While the thin films of PS_{140}–$PVBC_{140}$ readily converted to PS–PVBAC, the PS–PVBC thin films exhibited no observable microphase separation at any molar mass by AFM measurements or GISAXS analysis (Figures S51–S56). By AFM, the films were smooth, without any features observable in the height or phase measurements even when employing the intermodulation AFM technique (Figure 2a). Intermodulation AFM is useful for our experiments, as the cantilever tip is driven simultaneously at two different frequencies, which allows for the resolution of small differences in surface interactions between distinct domains. In addition, due to this method of driving the cantilever at two simultaneous frequencies, force and dissipation curves for each pixel within the AFM scan are generated simultaneously, which will be applied further below to aid in distinguishing unique domains within the material (for a more in-depth discussion of this technique and how it differs from typical AFM tapping mode techniques, please see the Supporting Information).[55] By GISAXS, no scattering peaks were observed outside of the Yoneda band (Figure S51). Small-angle X-ray scattering (SAXS) of the solvent cast bulk samples similarly showed no scattering peaks for any PS–PVBC sample (Figure S47). Furthermore, by DSC, we observed a single T_g for the diblock at 103 °C (Figure S44), similar to the behavior previously reported by Knauss and co-workers.[47] This behavior is most likely due to an exceedingly small Flory–Huggins interaction parameter, χ_{ij}, between PS and PVBC.

Because microphase separation was not observed for the PS–PVBC polymers, we attempted to increase the interaction parameter between our B and C blocks by replacing the proton at the 4 position of styrene with a chloride through the use of poly(4-chlorostyrene) (P4ClS) as an alternative neutral block. Unfortunately, there have been no previous studies of the solid-state behavior of block polymers containing P4ClS and PVBC. P4ClS–PVBC diblock polymers were synthesized by RAFT polymerization, first growing P4ClS from the CTA and then adding VBC onto the isolated and characterized P4ClS

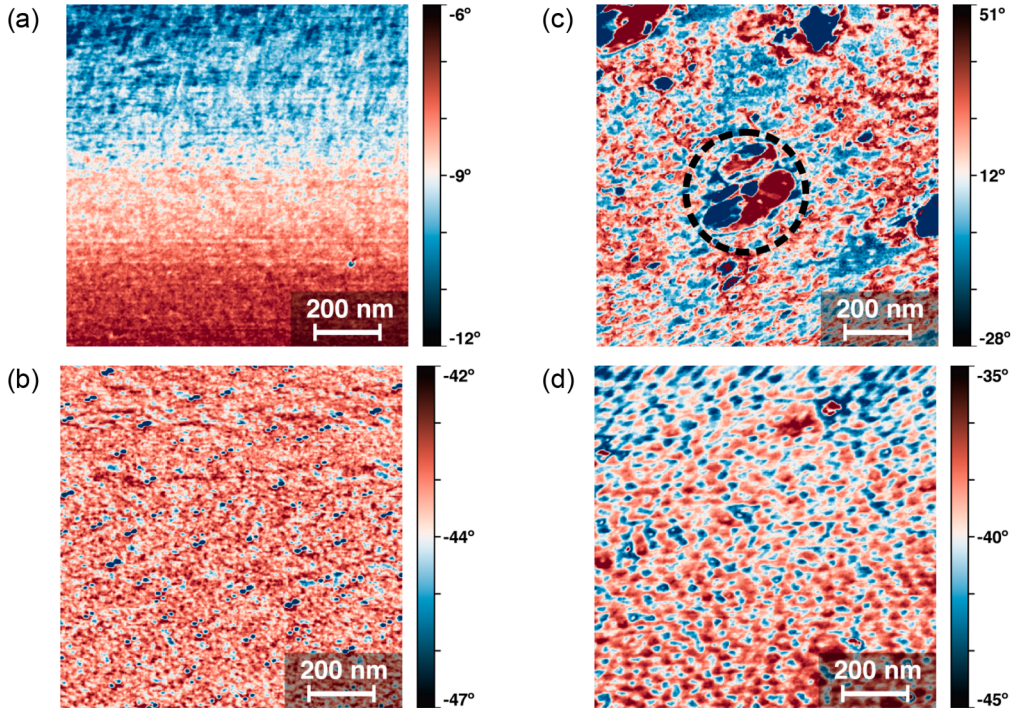

Figure 2. Intermodulation AFM phase images of (a) PS_{140}–$PVBC_{140}$, (b) $P4ClS_{700}$–$PVBC_{110}$, and (c) $PSSE_{260}$–$P4ClS_{1585}$ diblock polymers, as well as (d) $PSSE_{110}$–$P4ClS_{305}$–$PVBC_{70}$ triblock spin coated to make 50–70 nm films on bare silicon and solvent vapor annealed in chlorobenzene. In image 2a the apparent shift from blue to red is due to the inherent drift of the AFM tip over time during measurements. Image 2c has a few disordered features in the phase image such as the one highlighted with a black dashed circle, this is due to a large height defect on the surface, which can be seen in the overlay of height and phase images in the Supporting Information (Figure S68).

https://dx.doi.org/10.1021/acsapm.9b01100
ACS Appl. Polym. Mater. 2020, 2, 817–825

macroinitiator, yielding a diblock polymer P4ClS$_{700}$−PVBC$_{110}$ with M_n = 114 kg mol^{-1} and $Đ$ = 1.87 (Figures S14 and S30). By intermodulation AFM, we observed that the thin films of P4ClS$_{700}$−PVBC$_{110}$ exhibited circular domains ∼50 nm in diameter, both before and after solvent vapor annealing with chlorobenzene (Figure 2b). Upon exposure to TMA vapor for 1 h, the circular domains became more distorted and grew in size to 100 nm with "sticky", dissipative force curves, indicative of swollen alkyl ammonium domains (Figure S67). Because charged polymers can absorb humidity from the air, their water content is variable, which leads to changes in their T_g values. As a result, DSC data on the functionalized polyelectrolytes are inconsistent and cannot be used to help confirm microphase separation.[56] To further confirm the self-assembled morphology, we stained the TMA exposed films with an aqueous phosphotungstic acid ($H_3PW_{12}O_{40}$) solution and collected TEM images. The phosphotungstate is negatively charged, and therefore it should interact with the positively charged PVBAC domains and increase the contrast in the TEM image. We observed regularly spaced dark, circular domains around 80−100 nm in diameter (PVBAC) within a lighter matrix (P4ClS) (Figure 3). GISAXS experiments indicate that the domains

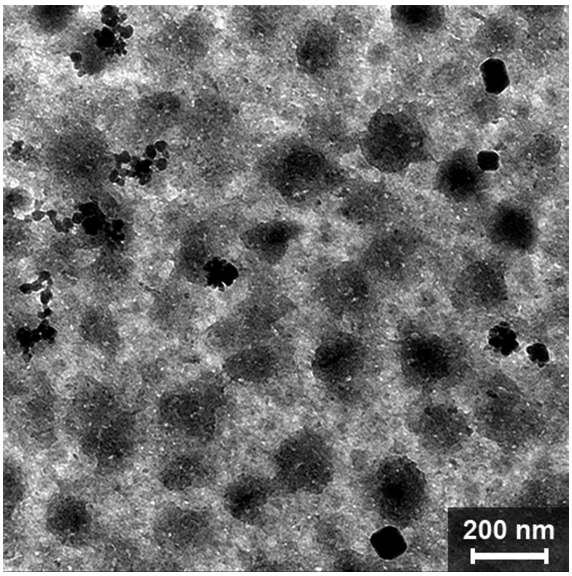

Figure 3. Transmission electron microscopy image of P4ClS$_{700}$−PVBC$_{110}$ 50 nm thick film after solvent vapor annealing with chlorobenzene and staining by submersion in a 0.1 wt % aqueous solution of phosphotungstic acid.

likely permeate through the film; a diffuse Bragg sheet scattering pattern is indicative of microphase separation of the two blocks within the film (Figure S57).

To determine the rate of the functionalization of PVBC in a P4ClS matrix, ATR-IR data were collected for a P4ClS$_{700}$−PVBC$_{110}$ diblock polymer film of 1 μm thickness (to increase the signal intensity) as a function of TMA exposure time. Figure 4 shows the IR band due to the C−Cl wag disappearance and the peak due to the C−N stretch appearance within an hour of TMA exposure, consistent with the S_N2 displacement of chloride by trimethylamine. GISAXS data of the "thick" films (>200 nm) indicate parallel features, suggesting that the morphology of the diblock polymer P4ClS$_{700}$−PVBC$_{110}$ films buries parallel PVBC layers at these thicknesses (Figure S57). As a result, we observe a slower

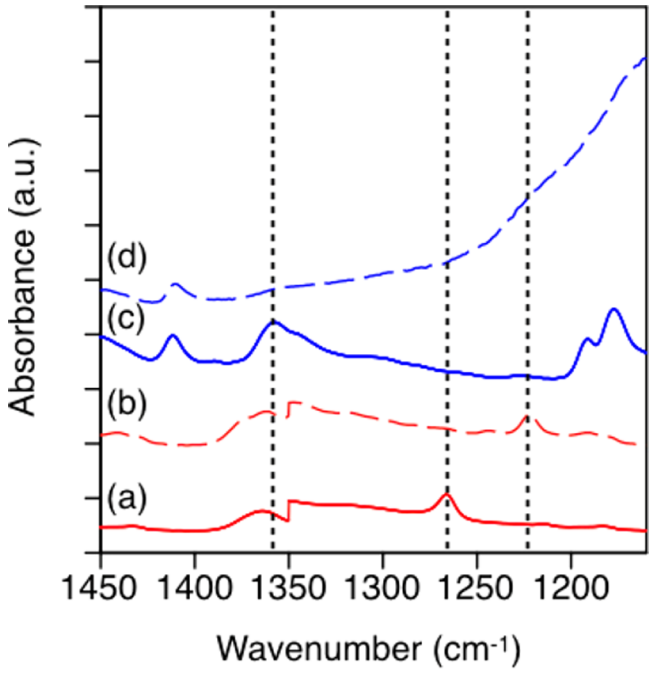

Figure 4. ATR-IR spectra of 1 μm thick films of diblock polymers P4ClS$_{700}$−PVBC$_{110}$ (a) before and (b) after 1 h of TMA exposure and PSSE$_{260}$-P4ClS$_{1585}$ (c) before and (d) after 12 h of TMA exposure. Black dashed lines are added to highlight the C−Cl wag at 1266 cm^{-1}, the C−N stretch at 1220 cm^{-1}, and the S═O stretch at 1357 cm^{-1}.

functionalization than that seen in a PVBC homopolymer because the domains are less accessible in the thicker films of the diblock polymers. In the thinner films that we used for morphological characterization (<100 nm), we identified perpendicularly oriented morphologies on the surface of our films in AFM, which likely increases the rate of the functionalization. From these results, we conclude that the P4ClS$_{700}$−PVBC$_{110}$ is microphase separated, and that the PVBC can be readily functionalized to the corresponding polycation under mild conditions.

Pre-Anionic Block. Our target polymer for the preanionic A block is poly(*n*-propyl styrene sulfonic ester) (PSSE), which can be converted to the polyanion poly(styrene sulfonate) (PSS) (Scheme 2).[57] PSS is a common polyelectrolyte, with uses in ion-exchange resins,[46] ion-exchange membranes for batteries,[58] and potassium binders for chronic kidney disease.[59] The initial *n*-propyl styrene sulfonic ester (SSE) monomer was synthesized according to literature methods by converting sodium styrene sulfate to the acid chloride and then condensing with *n*-propanol.[60−62] The SSE was then polymerized through RAFT polymerization using CTA and AIBN as a radical thermal initiator to form PSSE. Thermogravimetric analysis (Figure S33) showed a partial mass loss at ∼200 °C, which is consistent with literature reports of thermal alkyl deprotection of the sulfonic ester. Previously reported methods for deprotecting PSSE to PSS use a strong base to hydrolyze the ester group, such as sodium hydroxide.[57,62] Suspending the PSSE homopolymer in an aqueous solution of 30 wt % NaOH and heating to 70 °C led to deprotection of the sulfonic ester to the sulfonate, which could be monitored by FT-IR spectroscopy (Figure S64).

To confirm whether PSSE would microphase separate from P4ClS and to further confirm the sulfonic ester deprotection in a block copolymer, a PSSE macroinitiator was chain extended

https://dx.doi.org/10.1021/acsapm.9b01100
ACS Appl. Polym. Mater. 2020, 2, 817−825

with 4ClS in the presence of AIBN to yield a diblock polymer, $PSSE_{260}$–$P4ClS_{1585}$, with M_n = 225 kg mol^{-1} and $Đ$ = 1.15 (Figures S8 and S24). Polymer solutions were spin coated onto silicon wafers to produce 50 nm thick films (see SI for spin coating and annealing recipes), and intermodulation AFM was used to determine the microphase separated morphology of the thin film (Figure 2c). Again, disordered circular domains were observed, consistent with segregation of the two blocks. To verify that these nanoscale features permeated through the thin films, we measured the GISAXS of the $PSSE_{260}$–$P4ClS_{1585}$ thin films, which revealed perpendicular features with D spacing around 45 nm, in agreement with our observations by AFM (Figure S58).

During the course of these studies, various bases were evaluated for deprotecting the *n*-propyl sulfonic ester. We developed a strategy using an aqueous 45% solution of trimethylamine (TMA) (the same amine used to convert PVBC to the cationic block PVBAC). The conversion of PSSE to PSS in a 45% TMA aqueous solution was monitored by FT-IR spectroscopy of the isolated solid polymer after lyophilization, which showed full conversion after 8 h (Figure S65). Functionalization to the sulfonate in the solid state could also be achieved by simple exposure to TMA vapor in a sealed chamber. After 12 h of exposure to TMA vapor, we observed a quantitative conversion of $PSSE_{260}$–$P4ClS_{1585}$ to PSS_{260}–$P4ClS_{1585}$, as determined by ATR-IR spectroscopy, where the peak at 1357 cm^{-1} attributed to asymmetric S═O stretching of the sulfonic ester disappeared (Figure 4). GISAXS showed retention of the microphase separated morphologies with no observable change in the scattering pattern (Figure S59).

Triblock Polyampholytes. To obtain our desired microphase-separated anionic and cationic thin films, we targeted the synthesis of the neutral ABC triblock precursor poly(*n*-propyl styrene sulfonic ester)-*block*-poly(4-chlorostyrene)-*block*-poly(4-vinylbenzyl chloride) (PSSE–P4ClS–PVBC). As detailed above, the individual PSSE–P4ClS and P4ClS–PVBC diblock polymers displayed clear microphase separation behavior. The last step was to combine all three homopolymers into one ABC triblock terpolymer to ultimately obtain negative and positive domains within a neutral matrix. Starting with the $PSSE_{110}$–$P4ClS_{305}$ diblock polymer as the macroinitiator, PVBC was grown via RAFT polymerization to yield $PSSE_{110}$–$P4ClS_{305}$–$PVBC_{70}$ with M_n = 78 kg mol^{-1} and $Đ$ = 1.10 (Figures S15 and S31). Thermal analysis by DSC showed a single, merged T_g due to the small difference between the T_g values of the component polymers. A solution of the triblock polymer in chlorobenzene was spin coated onto native oxide silicon wafers to yield 68 nm thick films, which were solvent vapor annealed in chlorobenzene and then analyzed by intermodulation AFM. The phase image in Figure 2d shows circular domains on the order of 50 nm, illustrative of microphase separation of the polymer blocks. The domains were confirmed to permeate through the thickness of the film through GISAXS measurements (Figure S60).

Functionalization of the pre-anionic-*b*-neutral-*b*-pre-cationic triblock simultaneously to the anionic-*b*-neutral-*b*-cationic triblock polymer in the solid state was attempted by exposing the film to TMA vapor in a sealed chamber. The reaction progress was followed by ATR-IR spectroscopy, as previously detailed in the diblock polymer sections. However, the vibrational bands at 1270 cm^{-1}, indicative of the C–Cl wag, and at 1350 cm^{-1}, indicative of the S═O stretch of the sulfonate ester, did not decrease as a function of TMA exposure time (Figure S66).

Because the respective diblock polymers become fully functionalized in a short period of time, it seemed likely that there was some surface phenomenon preventing TMA from accessing the preanionic and precationic domains. To try to clean the surface, an unexposed sample of the polymer thin film was plasma etched with oxygen for 15 s, reducing the thickness from 68 to 57 nm. ATR-IR showed that the plasma etching did not result in the deprotection of the thin film. The etched film was then exposed to TMA vapor. ATR-IR showed complete functionalization of both the anionic A block and the cationic C block after 24 h of vapor exposure (Figure 5). We

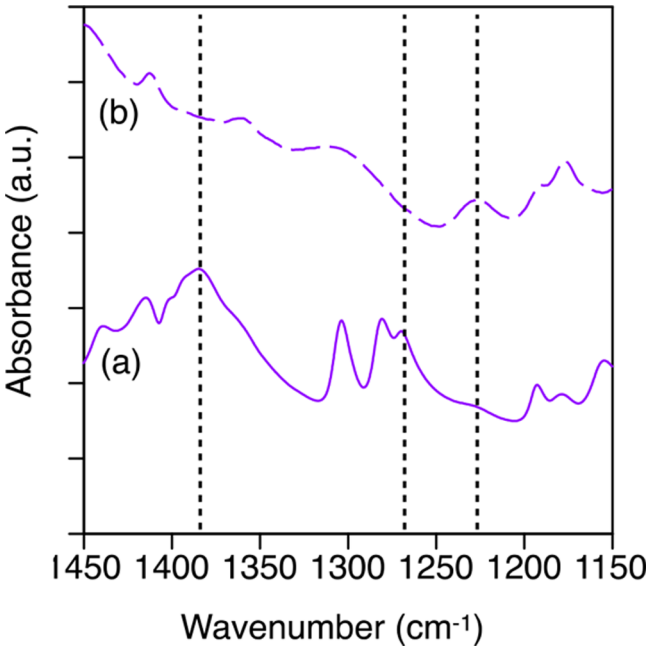

Figure 5. ATR-IR spectra of 57 nm thick films of plasma-etched triblock polymers $PSSE_{110}$–$P4ClS_{305}$–$PVBC_{70}$ (a) before (solid) and (b) after (dashed) exposure to TMA. Black dashed lines are added as guides for the eye to note the C–Cl wag at 1266 cm^{-1}, the C–N stretch at 1220 cm^{-1}, and the S═O stretch at 1357 cm^{-1}.

suspect that the surface energies lead to a thin layer of P4ClS that obscures the other blocks from functionalizing in the TMA vapor, but is thin enough that characterization shows the domains underneath the layer; a quick plasma etch treatment exposes the underlying layers that are then functionalized. AFM of the film after etching showed large height features, making the determination of the phase difference difficult (Figure S69), but after functionalization with TMA (Figure 6), the intermodulation AFM image was consistent with the microphase separation, confirming that the thin film maintains separate domains throughout the functionalization process. To further support this, we measured the force and dissipation curves of the microphase separated domains, revealing a softer red domain (the oscillation amplitude is higher, indicating that the tip pushes further into the material) consistent with the force curves of the PVBAC domains in the P4ClS–PVBAC diblock thin film (see Figure S67). Conversely, the blue domain is noticeably harder, consistent with these domains being comprised of different polymer blocks. We propose that the increase in the number of observable domains by AFM is a

https://dx.doi.org/10.1021/acsapm.9b01100
ACS Appl. Polym. Mater. 2020, 2, 817–825

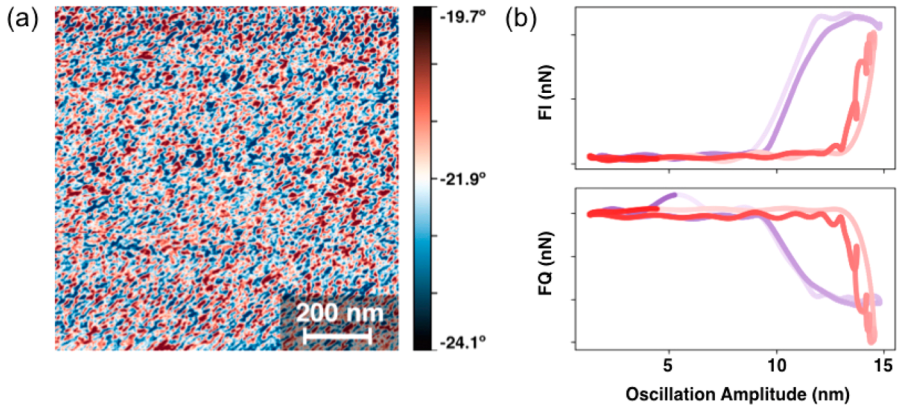

Figure 6. (a) Intermodulation AFM phase image of 57 nm thick film of $PSSE_{110}$−$P4ClS_{305}$−$PVBC_{70}$ triblock polymer after plasma etch and subsequent exposure to TMA vapor for 24 h. (b) Force (top) and dissipation (bottom) curves taken from a representative point within the blue domain (PSS, purple line) and red domain (PVBAC, red line).

result of the increased contrast due to the A and C blocks becoming charged and, therefore, having a greater interaction with the tip when compared to the previous glassy preionic blocks.

This novel single-step functionalization of PSSE−P4ClS−PVBC to simultaneously convert both preionic A and C blocks to anionic and cationic blocks, respectively, improves the ease of synthesis and fabrication compared to previous methods reported for multiblock functionalization.[16−18] Using TMA in the vapor phase, a convenient and mild base, allows a wider range of functional groups and side chains to be incorporated into the system without adverse side reactions that commonly occur when using harsh acids to convert polystyrene to poly(styrene sulfonate). The use of TMA also precludes the need for harsh, basic conditions previously employed to deprotect sulfonic esters to sulfonates in these polymer systems, e.g., 30 wt % NaOH at 70 °C for 2 days, which can lead to the decomposition of functional groups like esters to carboxylic acids, the degradation and corrosion of prefabricated membranes and silicon supports, or the chain scission of diblock polymers linked through ester linkages. Furthermore, the postfunctionalization purification now simply requires placing the films under vacuum to remove excess physisorbed TMA vapor, as opposed to washing or neutralization procedures. In previous work, these harsh conditions led to the loss of ordering in thin films of diblock and triblock polymers, the creation of holes in the membranes, and the need for BABCB pentablock polymers, where the neutral B block (polyisoprene) was cross-linked to immobilize the ionic domains.[16−18] Through this 2-in-1 functionalization, two synthetic steps and multiple purification steps are removed, resulting in an efficient and convenient way to achieve charged polymer domains using mild reagents. These factors mean the morphology of the thin films as well as any support structures are well maintained through the transformation.

CONCLUSION

Polyelectrolytes are used for a wide variety of applications, but their solid-state behavior has been relatively unexplored. We describe a combined method of fabrication for solid-state polyelectrolyte-containing thin films that uses a neutral triblock polymer to form microphase-separated morphologies. The polymers are then functionalized in a single step using mild reagents to yield a thin film containing spatially segregated positively and negatively charged domains. The domains are held together by a glassy poly(4-chlorostyrene) matrix that maintains the morphology of the film through the functionalization step. Conversion to poly(styrene sulfonate) as an anionic block and poly(4-vinylbenzyl trimethylammonium chloride) as a cationic block is easily monitored using ATR-IR spectroscopy and shown to reach quantitative conversion in thin films after exposure to TMA vapor. Finally, AFM and GISAXS show retention of the morphology before and after TMA vapor exposure. Future work on the solid-state morphology and its use in various applications will allow us to apply this simplified functionalization procedure. More efforts are needed in fabricating thin films with clear microphase-separated morphologies that maintain long-range order before and after functionalization. Further work can make use of this single step postpolymerization strategy with different B blocks that will allow for higher χ_{ij} parameters and different processing conditions, leading to thin films and bulk morphologies with long-range order and varying mechanical properties that can be tuned for a range of applications, including piezodialysis of wastewater and solid-state electrolytes for emerging battery technologies.

ASSOCIATED CONTENT

Supporting Information

The Supporting Information is available free of charge at https://pubs.acs.org/doi/10.1021/acsapm.9b01100.

Materials, instrumentation, experimental procedures, NMR spectra, SEC chromatograms, thermal analyses, SAXS scattering plots, GISAXS scattering plots, ATR-IR spectra of polymer functionalization, and AFM force curves (PDF)

AUTHOR INFORMATION

Corresponding Author

Marc A. Hillmyer − *Department of Chemistry, University of Minnesota, Minneapolis, Minnesota 55455, United States;* orcid.org/0000-0001-8255-3853; Email: hillmyer@umn.edu

Authors

David J. Goldfeld − *Department of Chemistry, University of Minnesota, Minneapolis, Minnesota 55455, United States;* orcid.org/0000-0002-9469-4319

https://dx.doi.org/10.1021/acsapm.9b01100
ACS Appl. Polym. Mater. 2020, 2, 817−825

Eric S. Silver − *Department of Chemistry, University of Minnesota, Minneapolis, Minnesota 55455, United States;* orcid.org/0000-0002-5957-9366

Madalyn R. Radlauer − *Department of Chemistry, University of Minnesota, Minneapolis, Minnesota 55455, United States;* orcid.org/0000-0002-3226-5340

Complete contact information is available at: https://pubs.acs.org/10.1021/acsapm.9b01100

Author Contributions

‡These authors contributed equally. The manuscript was written through contributions of all authors. All authors have given approval to the final version of the manuscript.

Funding

This work was supported by the National Science Foundation under DMR-1609459 and in part under DMR-1725272. M.R.R. held the Camille and Henry Dreyfus Foundation Postdoctoral Fellowship in Environmental Chemistry while performing this work.

Notes

The authors declare no competing financial interest.

■ ACKNOWLEDGMENTS

Parts of this work were carried out in the Characterization Facility, University of Minnesota, which receives partial support from the National Science Foundation (NSF) through the MRSEC program. The authors would like to acknowledge Greg Haugstad of the Characterization Facility, who contributed to the data collection methods involving intermodulation atomic force microscopy. Portions of this work were conducted in the Minnesota Nano Center, which is supported by the NSF through the National Nano Coordinated Infrastructure Network, Award Number NNCI-1542202. This research used resources of the Advanced Photon Source (APS), a U.S. Department of Energy (DOE) Office of Science User Facility operated for the DOE Office of Science by Argonne National Laboratory under Contract No. DE-AC02-06CH11357. The GISAXS data were obtained at the 8-ID-E beamline and analyzed by GIXSGUI software provided by the APS user facility.

■ ABBREVIATIONS

PS, polystyrene; VBC, vinylbenzyl chloride; PVBC, poly(vinylbenzyl chloride); PVBAC, poly(vinylbenzyl trialkylammonium chloride); SSE, *n*-propyl styrene sulfonic ester; PSSE, poly(*n*-propyl styrene sulfonic ester); 4ClS, 4-chlorostyrene; P4ClS, poly(4-chlorostyrene); PSS, poly(styrene sulfonate); TMA, trimethylamine; AIBN, azobisisobutyronitrile; AFM, atomic force microscopy; ATR-IR, attenuated total reflectance infrared spectroscopy; SAXS, small-angle X-ray scattering; GISAXS, grazing-incidence small-angle X-ray scattering; TEM, transmission electron microscopy; CTA, chain transfer agent (4-cyano-4-[(dodecylsulfanylthiocarbonyl)sulfanyl]pentanoic acid); FTIR, Fourier-transform infrared spectroscopy

■ REFERENCES

(1) Pinto, M. R.; Schanze, K. S. Conjugated Polyelectrolytes: Synthesis and Applications. *Synthesis* **2002**, *9*, 1293−1309.

(2) Freyer, J. L.; Brucks, S. D.; Campos, L. M. Fully charged: Maximizing the potential of cationic polyelectrolytes in applications ranging from membranes to gene delivery through rational design. *J. Polym. Sci., Part A: Polym. Chem.* **2017**, *55*, 3167−3174.

(3) Zhang, W.; Zhao, Q.; Yuan, J. Porous Polyelectrolytes: The Interplay of Charge and Pores for New Functionalities. *Angew. Chem., Int. Ed.* **2018**, *57*, 6754−6773.

(4) Zhao, Q.; An, Q. F.; Ji, Y.; Qian, J.; Gao, C. Polyelectrolyte complex membranes for pervaporation, nanofiltration and fuel cell applications. *J. Membr. Sci.* **2011**, *379*, 19−45.

(5) Scranton, A. B.; Rangarajan, B.; Klier, J. *Biomedical Applications of Polyelectrolytes*; Springer-Verlag: Berlin, Germany, 1995; Vol. *122*.

(6) Bronich, T. K.; Kabanov, A. V.; Kabanov, V. A.; Yu, K.; Eisenberg, A. Soluble Complexes from Poly(ethylene oxide)-*block*-polymethacrylate Anions and *N*-Alkylpyridinium Cations. *Macromolecules* **1997**, *30*, 3519−3525.

(7) Hunt, J. N.; Feldman, K. E.; Lynd, N. A.; Deek, J.; Campos, L. M.; Spruell, J. M.; Hernandez, B. M.; Kramer, E. J.; Hawker, C. J. Tunable, high modulus hydrogels driven by ionic coacervation. *Adv. Mater.* **2011**, *23*, 2327−2331.

(8) Nowak, A. P.; Breedveld, V.; Pakstis, L.; Ozbas, B.; Pine, D. J.; Pochan, D.; Deming, T. J. Rapidly recovering hydrogel scaffolds from self-assembling diblockcopolypeptide amphiphiles. *Nature* **2002**, *417*, 424−428.

(9) Raviv, U.; Glasson, S.; Kampf, N.; Gohy, J.-F.; Jérôme, R.; Klein, J. Lubrication by charged polymers. *Nature* **2003**, *425*, 163−165.

(10) Gucht, J. v. d.; Spruijt, E.; Lemmers, M.; Cohen Stuart, M. A. Polyelectrolyte complexes: bulk phases and colloidal systems. *J. Colloid Interface Sci.* **2011**, *361*, 407−422.

(11) Kimerling, A. S.; Rochefort, W. E.; Bhatia, S. R. Rheology of Block Polyelectrolyte Solutions and Gels: A Review. *Ind. Eng. Chem. Res.* **2006**, *45*, 6885−6889.

(12) Delaney, K. T.; Fredrickson, G. H. Theory of polyelectrolyte complexation−Complex coacervates are self-coacervates. *J. Chem. Phys.* **2017**, *146*, 224902.

(13) Yang, S.; Vishnyakov, A.; Neimark, A. V. Self-assembly in block polyelectrolytes. *J. Chem. Phys.* **2011**, *134*, 054104.

(14) Lowe, A. B.; McCormick, C. L. Synthesis and Solution Properties of Zwitterionic Polymers. *Chem. Rev.* **2002**, *102*, 4177−4190.

(15) Dobrynin, A. V.; Colby, R. H.; Rubinstein, M. Polyampholytes. *J. Polym. Sci., Part B: Polym. Phys.* **2004**, *42*, 3513−3538.

(16) Isono, Y.; Tanisugi, H.; Endo, K.; Fujimoto, T.; Hasegawa, H.; Hashimoto, T.; Kawai, H. Morphological and Mechanical Properties of Multiblock Copolymers. *Macromolecules* **1983**, *16*, 5−10.

(17) Fujimoto, T.; Ohkoshi, K.; Miyaki, Y.; Nagasawa, M. A New Charge-Mosaic Membrane from a Multiblock Copolymer. *Science* **1984**, *224*, 74−76.

(18) Miyaki, Y.; Iwata, M.; Fujita, Y.; Tanisugi, H.; Isono, Y.; Fujimoto, T. Artificial Membranes from Multiblock Copolymers. 2. Molecular Characterization and Morphological Behavior of Pentablock Copolymers of the ISIAI Type. *Macromolecules* **1984**, *17*, 1907−1912.

(19) Mendes, P. M.; Yeung, C. L.; Preece, J. A. Bio-nanopatterning of Surfaces. *Nanoscale Res. Lett.* **2007**, *2*, 373−384.

(20) Gao, P.; Hunter, A.; Summe, M. J.; Phillip, W. A. A Method for the Efficient Fabrication of Multifunctional Mosaic Membranes by Inkjet Printing. *ACS Appl. Mater. Interfaces* **2016**, *8*, 19772−19779.

(21) Rajesh, S.; Yan, Y.; Chang, H.-C.; Gao, H.; Phillip, W. A. Mixed Mosaic Membranes Prepared by Layer-by-Layer Assembly for Ionic Separations. *ACS Nano* **2014**, *8*, 12338−12345.

(22) Higa, M.; Masuda, D.; Kobayashi, E.; Nishimura, M.; Sugio, Y.; Kusudou, T.; Fujiwara, N. Charge mosaic membranes prepared from laminated structures of PVA-based charged layers: 1. Preparation and transport properties of charged mosaic membranes. *J. Membr. Sci.* **2008**, *310*, 466−473.

(23) Bates, F. S.; Fredrickson, G. H. Block Copolymers—Designer Soft Materials. *Phys. Today* **1999**, *52*, 32−38.

(24) Albert, J. N. L.; Epps, T. H. Self-assembly of block copolymer thin films. *Mater. Today* **2010**, *13*, 24−33.

(25) Luo, M.; Epps, T. H. Directed Block Copolymer Thin Film Self-Assembly: Emerging Trends in Nanopattern Fabrication. *Macromolecules* **2013**, *46*, 7567−7579.

(26) Segalman, R. A. Patterning with block copolymer thin films. *Mater. Sci. Eng., R* **2005**, *48*, 191−226.
(27) Choi, J.; Huh, J.; Carter, K. R.; Russell, T. P. Directed Self-Assembly of Block Copolymer Thin Films Using Minimal Topographic Patterns. *ACS Nano* **2016**, *10*, 7915−7925.
(28) Laschewsky, A. Structures and Synthesis of Zwitterionic Polymers. *Polymers* **2014**, *6*, 1544−1601.
(29) Philipp, B.; Dautzenberg, H.; Linow, K.-J.; Kötz, J.; Dawydoff, W. Polyelectrolyte Complexes - Recent Developments and Open Problems. *Prog. Polym. Sci.* **1989**, *14*, 91−172.
(30) Wang, Q.; Schlenoff, J. B. The Polyelectrolyte Complex/Coacervate Continuum. *Macromolecules* **2014**, *47*, 3108−3116.
(31) Ahmed, L. S.; Xia, J.; Dubin, P. L.; Kokufuta, E. Stoichiometry and the Mechanism of Complex Formation in Protein-Polyelectrolyte Coacervation. *J. Macromol. Sci., Part A: Pure Appl.Chem.* **1994**, *31*, 17−29.
(32) Chollakup, R.; Smitthipong, W.; Eisenbach, C. D.; Tirrell, M. Phase Behavior and Coacervation of Aqueous Poly(acrylic acid)-Poly(allylamine) Solutions. *Macromolecules* **2010**, *43*, 2518−2528.
(33) Antonov, M.; Mazzawi, M.; Dubin, P. L. Entering and Exiting the Protein−Polyelectrolyte Coacervate Phase via Nonmonotonic Salt Dependence of Critical Conditions. *Biomacromolecules* **2010**, *11*, 51−59.
(34) Qin, J.; Priftis, D.; Farina, R.; Perry, S. L.; Leon, L.; Whitmer, J.; Hoffmann, K.; Tirrell, M.; de Pablo, J. J. Interfacial Tension of Polyelectrolyte Complex Coacervate Phases. *ACS Macro Lett.* **2014**, *3*, 565−568.
(35) Kelly, K. D.; Schlenoff, J. B. Spin-Coated Polyelectrolyte Coacervate Films. *ACS Appl. Mater. Interfaces* **2015**, *7*, 13980−13986.
(36) Tang, C.; Sivanandan, K.; Stahl, B. C.; Fredrickson, G. H.; Kramer, E. J.; Hawker, C. J. Multiple Nanoscale Templates by Orthogonal Degradation of a Supramolecular Block Copolymer Lithographic System. *ACS Nano* **2010**, *4*, 285−291.
(37) Guliyeva, A.; Vayer, M.; Warmont, F.; Faugère, A. M.; Andreazza, P.; Takano, A.; Matsushita, Y.; Sinturel, C. Thin Films with Perpendicular Tetragonally Packed Rectangular Rods Obtained from Blends of Linear ABC Block Terpolymers. *ACS Macro Lett.* **2018**, *7*, 789−794.
(38) Tang, C.; Lennon, E. M.; Fredrickson, G. H.; Kramer, E. J.; Hawker, C. J. Evolution of Block Copolymer Lithography to Highly Ordered Square Arrays. *Science* **2008**, *322*, 429−432.
(39) Malhotra, S. L.; Lessard, P.; Minh, L.; Blanchard, L. P. Thermal Decomposition and Glass-Transition Temperature Study of Poly-*p*-methylstyrene. *J. Macromol. Sci., Chem.* **1980**, *14*, 517−540.
(40) Malhotra, S. L.; Lessard, P.; Blanchard, L. P. The Thermal Decomposition and Glass Transition Temperature of Poly(p-tert-butylstyrene). *J. Macromol. Sci., Chem.* **1981**, *A15*, 121−141.
(41) Thermal Transitions of Homopolymers: Glass Transition & Melting Point. https://www.sigmaaldrich.com/technical-documents/articles/materials-science/polymer-science/thermal-transitions-of-homopolymers.html (accessed June 7, 2019).
(42) Thunhorst, K. L.; Noble, R. D.; Bowman, C. N., Preparation of Functionalized Polymers by Reactions of Poly(Vinylbenzyl Chloride). In *Polymer Modification*; Swift, G., Carraher, C. E., Jr., Bowman, C. N., Eds.; Plenum Publishing: New York, NY, 1997; pp 97−107.
(43) Ting, W.-H.; Dai, S. A.; Shih, Y.-F.; Yang, I. K.; Su, W.-C.; Jeng, R.-J. Facile synthetic route toward poly(vinyl benzyl amine) and its versatile intermediates. *Polymer* **2008**, *49*, 1497−1505.
(44) Haladjova, E.; Mountrichas, G.; Pispas, S.; Rangelov, S. Poly(vinylbenzyl trimethylammonium chloride) Homo and Block Copolymers Complexation with DNA. *J. Phys. Chem. B* **2016**, *120*, 2586−2595.
(45) Lloyd, W. G.; Durocher, T. E. Nucleophilic Displacements upon Poly(vinylbenzyl chloride). *J. Appl. Polym. Sci.* **1963**, *7*, 2025−2033.
(46) Alexandratos, S. D. Ion-Exchange Resins: A Retrospective from Industrial and Engineering Chemistry Research. *Ind. Eng. Chem. Res.* **2009**, *48*, 388−398.
(47) Li, Y.; Jackson, A. C.; Beyer, F. L.; Knauss, D. M. Poly(2,6-dimethyl-1,4-phenylene oxide) Blended with Poly(vinylbenzyl chloride)-*b*-polystyrene for the Formation of Anion Exchange Membranes. *Macromolecules* **2014**, *47*, 6757−6767.
(48) Cao, Y.-C.; Wang, X.; Mamlouk, M.; Scott, K. Preparation of alkaline anion exchange polymer membrane from methylated melamine grafted poly(vinylbenzyl chloride) and its fuel cell performance. *J. Mater. Chem.* **2011**, *21*, 12910−12916.
(49) Moad, G.; Rizzardo, E.; Thang, S. H. Radical addition−fragmentation chemistry in polymer synthesis. *Polymer* **2008**, *49*, 1079−1131.
(50) Couture, G.; Améduri, B. Kinetics of RAFT homopolymerisation of vinylbenzyl chloride in the presence of xanthate or trithiocarbonate. *Eur. Polym. J.* **2012**, *48*, 1348−1356.
(51) Merrifield, R. B. The Synthesis of a Tetrapeptide. *J. Am. Chem. Soc.* **1963**, *85*, 2149−2154.
(52) Wang, X.; Goswami, M.; Kumar, R.; Sumpter, B. G.; Mays, J. Morphologies of block copolymers composed of charged and neutral blocks. *Soft Matter* **2012**, *8*, 3036−3052.
(53) Hickner, M. A.; Herring, A. M.; Coughlin, E. B. Anion exchange membranes: Current status and moving forward. *J. Polym. Sci., Part B: Polym. Phys.* **2013**, *51* (24), 1727−1735.
(54) Lacroix-Desmazes, P.; Delair, T.; Pichot, C.; Boutevin, B. Synthesis of Poly(chloromethylstyrene-*b*-styrene) Block Copolymers by Controlled Free-Radical Polymerization. *J. Polym. Sci., Part A: Polym. Chem.* **2000**, *38* (21), 3845−3854.
(55) Haviland, D. B. Quantitative force microscopy from a dynamic point of view. *Curr. Opin. Colloid Interface Sci.* **2017**, *27*, 74−81.
(56) Zhang, Y.; Batys, P.; O'Neal, J. T.; Li, F.; Sammalkorpi, M.; Lutkenhaus, J. L. *ACS Cent. Sci.* **2018**, *4*, 638−644.
(57) Chen, L.; Hallinan, D. T., Jr.; Elabd, Y. A.; Hillmyer, M. A. Highly Selective Polymer Electrolyte Membranes from Reactive Block Polymers. *Macromolecules* **2009**, *42*, 6075−6085.
(58) Higgins, T. M.; Park, S. H.; King, P. J.; Zhang, C. J.; McEvoy, N.; Berner, N. C.; Daly, D.; Shmeliov, A.; Khan, U.; Duesberg, G.; Nicolosi, V.; Coleman, J. N. A Commercial Conducting Polymer as Both Binder and Conductive Additive for Silicon Nanoparticle-Based Lithium-Ion Battery Negative Electrodes. *ACS Nano* **2016**, *10*, 3702−3713.
(59) Hunt, T. V.; DeMott, J. M.; Ackerbauer, K. A.; Whittier, W. L.; Peksa, G. D. Single-dose sodium polystyrene sulfonate for hyperkalemia in chronic kidney disease or end-stage renal disease. *Clin. Kidney J.* **2019**, *12*, 408−413.
(60) Schuh, K.; Prucker, O.; Rühe, J. Surface Attached Polymer Networks through Thermally Induced Cross-Linking of Sulfonyl Azide Group Containing Polymers. *Macromolecules* **2008**, *41*, 9284−9289.
(61) Kolomanska, J.; Johnston, P.; Gregori, A.; Fraga Domínguez, I.; Egelhaaf, H.-J.; Perrier, S.; Rivaton, A.; Dagron-Lartigau, C.; Topham, P. D. Design, synthesis and thermal behaviour of a series of well-defined clickable and triggerable sulfonate polymers. *RSC Adv.* **2015**, *5*, 66554−66562.
(62) Lienkamp, K.; Schnell, I.; Groehn, F.; Wegner, G. Polymerization of Styrene Sulfonate Ethyl Ester by ATRP: Synthesis and Characterization of Macromonomers for Suzuki Polycondensation. *Macromol. Chem. Phys.* **2006**, *207*, 2066−2073.

https://dx.doi.org/10.1021/acsapm.9b01100
ACS Appl. Polym. Mater. 2020, 2, 817−825